Effect of sphingomyelin and cholesterol on the interaction of St II with lipidic interfaces

ARTICLE *in* TOXICON · FEBRUARY 2007

Impact Factor: 2.49 · DOI: 10.1016/j.toxicon.2006.09.019 · Source: PubMed

ELSEVIER

Toxicon 49 (2007) 68–81

TOXICON

www.elsevier.com/locate/toxicon

Effect of sphingomyelin and cholesterol on the interaction of St II with lipidic interfaces

Diana Martínez[a,*], Anabel Otero[a], Carlos Alvarez[a,b], Fabiola Pazos[a], Mayra Tejuca[a], María Eliana Lanio[a], Ion Gutiérrez-Aguirre[c], Ariana Barlic[c], Ibon Iloro[c], Jose Luis Arrondo[c], Juan Manuel González-Mañas[c], Eduardo Lissi[d]

[a]*Facultad de Biología, Universidad de la Habana, Centro de Estudio de Proteínas, Calle 25 no 455, CP 10400, Cuba*
[b]*Instituto de Química, Universidade de São Paulo, SP, Brasil*
[c]*Unidad de Biofísica (CSIC-UPV/EHU) and Departamento de Bioquímica y Biología Molecular, Universidad del País Vasco, Apartado 644, 48080 Bilbao, España*
[d]*Departamento de Química, Facultad de Química y Biología, Universidad de Santiago de Chile, P.O. Box 40, Santiago de Chile, Santiago 33, Chile*

Received 13 April 2006; received in revised form 13 September 2006; accepted 15 September 2006
Available online 29 September 2006

Abstract

Sticholysin II (St II) is a cytolysin produced by the sea anemone *Stichodactyla helianthus*, characterized by forming oligomeric pores in natural and artificial membranes. In the present work the influence of the membrane lipidic components sphingomyelin (SM) and cholesterol (Cho) on binding and functional activity of St II, was evaluated using ELISA, lipid monolayers and liposomes. The aim of this work was to establish the promoting role of Cho and SM, both in St II binding and pore formation efficiency. In general the association (evaluated by ELISA and incorporation to phospholipid monolayers) of St II to lipids mixtures was better than to any one of the single components. Regarding the unique role of SM, it was found that, albeit inefficiently, St II binds to phosphatidylcholine (PC):Cho monolayers and liposomes, and is able to form active pores in these bilayers. The results in monolayers and liposomes show that the presence of SM and large amounts of Cho leads to the highest values of critical pressure and rate of association to monolayers, the most favorable interaction with liposomes, and the fastest rate of pore formation, in spite of the rigidity of the layers as suggested by the high generalized polarization (GP) of Laurdan incorporated to liposomes and FTIR data. Taken together, the present results show that the joint presence of SM and Cho, both in binary and ternary (PC containing) mixtures provide conditions particularly suitable for St II binding and function. We suggest that microdomains present in the bilayers could be important for toxin-membrane association.

Keywords: Sticholysin; Cholesterol; Sphingomyelin; Monolayers; Pore-forming toxin; Vesicle permeabilization

1. Introduction

Sticholysin II (St II) (SwissProt accession number: P077845) is the major and most hemolytic cytolysin purified from the sea anemone

*Corresponding author. Fax: +53 7 8321321.
E-mail address: dmcb@fbio.uh.cu (D. Martínez).

0041-0101/$ - see front matter © 2006 Elsevier Ltd. All rights reserved.
doi:10.1016/j.toxicon.2006.09.019

Stichodactyla helianthus (Lanio et al., 2001). The first purification and partial sequencing of this toxin-former *Stiochactis* cytolysin III (C-III)-was performed by Blumental and Kem (1983). Later, Stevens et al. (2002) demonstrated that St II and C-III correspond to the same protein obtained by two alternative purification procedures.

St II belongs to the group of highly homologous proteins known as actinoporins. These proteins bind to biological and model membranes forming oligomeric pores of ca. 1 nm internal hydrodynamic radius (Tejuca et al., 2001; Anderluh and Maček, 2002). Toxin binding to model membranes, as well as the reversibility of the process and its pore formation efficiency, are strongly influenced by the presence of sphingomyelin (SM) (Tejuca et al., 1996; Caaveiro et al., 2001). The special role of SM in association of sticholysins with membranes was first demonstrated by Bernheimer and Avigad (1976) and Linder et al. (1977). The equimolar phosphatidylcholine (PC):SM vesicles are considered very good targets for these proteins (Tejuca et al., 1996; Alvarez-Valcárcel et al., 2001). However, sticholysin pores can be formed in bilayers lacking SM (Shin et al., 1979; De los Ríos et al., 1998). Furthermore, it has been shown that the hemolytic activity (HA) of actinoporins on red blood cells from different species is not related to the proportion of any specific lipid present in the membrane (Doyle and Kem, 1989; Macek et al., 1994). These results would argue against a unique role for SM in the pore forming capacity of the toxin.

Anemone cytolysins can be considered as potential tools for the construction of immunoconjugates selectively addressed to parasite and tumoral cells (Tejuca et al., 1999, 2004). In order to better understand basic aspects of the interaction between these toxins and lipidic interfaces, studies were performed regarding St II interaction with several lipidic systems (ELISA, lipid monolayers and unilamellar vesicles). The main lipid components of erythrocyte membrane (PC, SM and Cho) were combined in binary and ternary mixtures, in order to analyze the effect of the membrane composition upon St II binding affinity and pore formation capacity. These studies would contribute to a better understanding of the association and organization of these toxins into membranes and are essential for the rational design of immunotoxins.

2. Materials and methods

2.1. Materials

St II (Swiss Protein Data Bank PO7845) was purified from the sea anemone *S. helianthus* as previously described by Lanio et al. (2001). The protein concentration was determined using an absorption coefficient at 280 nm of 1.87 mL $mg^{-1}\,cm^{-1}$ (Lanio et al., 2001). Brain SM and egg PC were purchased from Avanti Polar Lipids, and cholesterol (Cho) was from Sigma. 8-Aminonaphtalene-1,3,6-trisulfonic acid (ANTS), Laurdan (6-lauroyl-2-dimethylamino naphthalene), and *p*-xylene-bis-pyridiumbromide (DPX) were from Molecular Probes. The rabbit IgG fraction anti-St II antiserum was obtained and purified by the Laboratory of Immunology of the Faculty of Biology, University of Havana.

2.2. ELISA with lipidic coat

St II binding to various lipids was evaluated by ELISA, as described previously (Yamaji et al., 1998). In brief, Costar microtiter plates were coated with an appropriate amount of lipid (0.4 nmol) dissolved in ethanol by evaporation of the solvent overnight at room temperature (~25 °C). After blocking with phosphate buffer (PBS: Na_2HPO_4 9.6 mM, NaCl 137 mM, KCl 2.7 mM, KH_2PO_4 1.47 mM, pH 7.2) containing 3% BSA during 60 min to avoid unspecific interactions, the plates were incubated with various concentrations of St II (0.62–15 nM) in PBS–BSA 1% for 1 h at 37 °C. After washing five times with PBS–BSA 1%, the bound protein was detected incubating the plates for 1 h at 37 °C with 0.1 mL of rabbit IgG fraction anti-St II antiserum (Pico et al., 2004), diluted 1/2100 with PBS–BSA 1%, and followed by incubation (90 min at 37 °C) with anti-rabbit IgG and peroxidase conjugate. The intensity of the color developed with *o*-phenylenediamine was measured at 492 nm using a Multiscan EX reader (Labsystems, Finland). Control experiments were carried out to discard the blockage of toxin–lipid interaction by BSA.

2.3. Surface pressure measurements

Surface pressure measurements were carried out with μThrough-S system from Kibrom (Helsinki, Finland) at 25 °C employing plates of ca. 3.14 cm^2.

The aqueous phase consisted of 1 mL of 10 mM Hepes, 200 mM NaCl, pH 7.5. Samples of pure lipids or lipid mixtures of appropriate compositions, dissolved in chloroform:methanol (2:1), were gently spread over the surface, and the desired initial surface pressure attained by changing the amount of lipid applied to the air–water interface. The protein was injected through a hole connected to the subphase. The final protein concentration was 0.93 μM. The increment in surface pressure was recorded under constant stirring, as a function of the elapsed time, until a stable signal was obtained. The maximum attainable pressure of the lipids was evaluated by registering the surface pressure after addition of increasing amounts of lipids to the air–water interface of the buffer solution.

2.4. Vesicle preparation

The appropriate amounts of lipids dissolved in the organic solvent (chloroform:methanol 2:1 v/v) were mixed and evaporated thoroughly at 50 °C. Multilamellar vesicles (MLV) were prepared by hydration of the lipid film with buffer, intensive vortexing and heating at 50 °C. Large unilamellar vesicles (LUV) were prepared by the extrusion method (Mayer et al., 1986), submitting the MLV to 10 freezing/thawing cycles and 10 extrusion cycles (50 °C) through polycarbonate filters with a pore size of 0.1 μM (Nucleopore, USA). Liposomes for fluorescence experiments were prepared in 10 mM Hepes, 200 mM NaCl, pH 7.5. Vesicles with encapsulated solutes were prepared in a solution containing 10 mM Hepes, 25 mM ANTS, 90 mM DPX, and 50 mM NaCl, pH 7.5. Non-encapsulated fluorescent probes were removed from the vesicle suspension passaging them through a Sephadex G-75 gel filtration column under isosmotic conditions. Solution osmolarities were measured using an Osmomat 030 instrument (Gonotec, Germany). Phospholipid and Cho concentrations were determined as previously described (Bartlett, 1959; Kates, 1972) and with a kit purchased to Merck (1.14830.0001), respectively. The average size and polydispersity (lower than 0.2) of the vesicles were measured by quasi-elastic light scattering in a Zetasizer 4 photometer (Malvern Instruments, UK). Small unilamellar vesicles (SUV) were prepared by sonication of the MLV (2 min total time, cycles of 15 s sonication with intervals of 15 s). Disruption of the MLV was assessed by the decrease in turbidity.

2.5. Binding of St II to liposomes

Binding of St II to liposomes was assessed by measuring the HA of filtrates after ultrafiltration of St II-LUVs solutions using Centrisart I Units (Sartorious). Filters were washed with a solution comprising 1% BSA. Control experiments carried out in absence of liposomes showed that, under these conditions, no St II is retained by the filters. Centrifugation was carried out at 600*g* during 5 min. The remaining HA (%) in the ultrafiltrate was evaluated according to Martínez et al. (2001), and equated to the fraction of unbound toxin. The reversibility of the process was assessed by measuring the effect of St II pre-incubation (10 min) with SUVs upon the toxin HA (Alvarez-Valcárcel et al., 2001).

2.6. Fluorescence measurements

Fluorescence measurements were carried out in a Spex Fluorolog spectrofluorimeter (USA), equipped with a constant temperature cell holder. Excitation and emission slits were 2.5 and 5 nm, respectively. Protein samples, at a final concentration 0.7 μM, were excited at 295 nm and the fluorescence measured at 335 nm, in order to minimize tyrosine emission (Lakowicz, 1999). To this solution, increasing amounts of SUV were added, and the change in fluorescence intensity was measured. The dilution of the sample and the dispersion associated to the vesicles were corrected employing tryptophan fluorescence as reference. Some measurements were also carried out with larger St II concentrations (1.4 and 2.8 μM). Quenching experiments employing acrylamide were performed in buffer solution and in the presence of lipids (120 μM).

Laurdan fluorescence was employed in order to estimate the phase state of the liposomes. Generalized polarization (GP) determinations were performed at 25 °C, according to the procedure proposed by Parasassi et al. (1990):

$$GP = (I_{440} - I_{490})/(I_{440} + I_{490}), \quad (1)$$

where I_{440} and I_{490} are the fluorescence intensities measured at the corresponding wavelengths after excitation at 340 nm. Experiments were performed employing 2.6 mM total lipids and a lipid/probe ratio of 500.

The membrane fluidity was also assessed by Fourier transform infrared spectroscopy (FTIR). LUVs were prepared in deuterated buffer,

Hepes-D_2O 10 mM, 200 mM NaCl, pD 7.5. The samples were placed in a thermostated cell with CaF_2 windows and IR spectra recorded in a Nicolet Magna 550 spectrophotometer equipped with a mercury–cadmium–tellurium detector. The procedure was similar to that reported by Caaveiro et al. (2001). The phase state of the bilayer was estimated measuring the maximum of the band corresponding to the vibrations of CH_2 (centered at 2800–2880 cm^{-1}) groups of the lipid acyl chains (Muga et al., 1991).

2.7. Permeabilization assays

The leakage of encapsulated solutes was assayed as described by Ellens et al. (1985) using ANTS as fluorophore and DPX as quencher. Probe-loaded liposomes (final concentration 0.1 mM in lipids) were treated with the appropriate amounts of toxin at 25 °C under constant stirring. Changes in fluorescence intensity were recorded in a SLM AMINCO MC-200 (USA) spectrofluorimeter with excitation and emission wavelengths set at 355 and 530 nm, respectively. An interference filter, with a nominal cutoff value of 475 nm, was placed in the emission light path to minimize the contribution of the scattered-light from the vesicles to the fluorescence signal. The fraction of permeabilized vesicles was calculated after addition of a large excess of protein.

3. Results and discussion

3.1. Association of St II to lipidic layers evaluated by ELISA

In order to evaluate the affinity of the toxin towards the main lipid constituents of the external monolayer of the red cell membrane (PC, SM and Cho), binding assays were performed employing an ELISA that provides information regarding the capacity of the corresponding lipid to irreversibly bind the protein.

Plates were covered with equivalent molar amounts of the lipids, and the amount of protein retained was evaluated as a function of the added protein concentration. The results obtained are shown in Fig. 1(A). The continuous lines correspond to data best fit of the Langmuir's isotherms:

$$y = (A_{max}x)/(1 + P_{50}x), \quad (2)$$

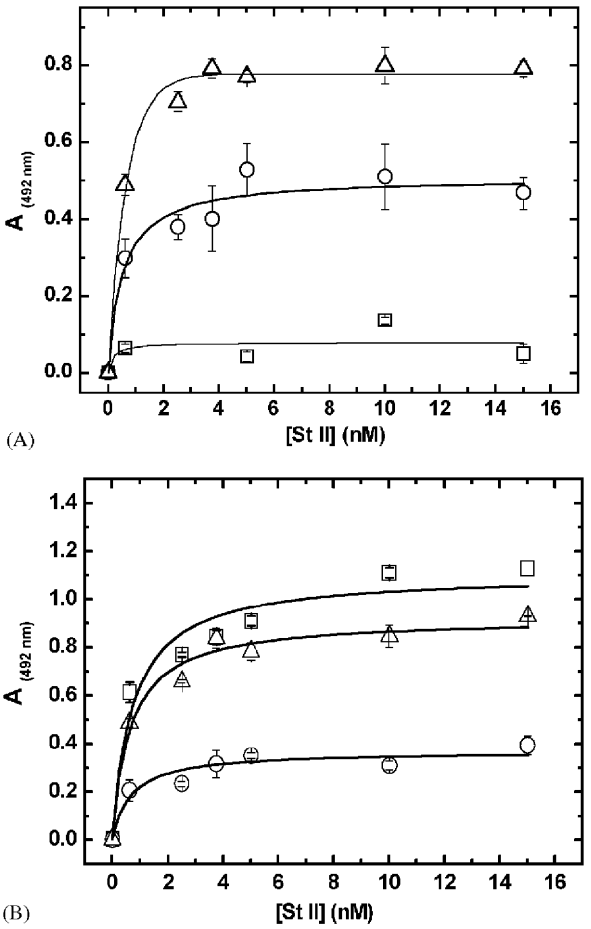

Fig. 1. (A) Extent of irreversible binding of St II to single lipids. Absorbance at 492 nm in ELISA, reported as a function of the St II concentration in the solution. Lipid amount: 0.4 nmol per assay. Each point corresponds to the average of three independent experiments, and the bars indicate their standard deviation. Deposited lipid: (□) Cholesterol; (○) PC and (Δ) SM. The lines show the best fit hyperboles; (B) extent of irreversible St II binding to equimolar binary lipid mixtures. The conditions were similar to those given in (A). Deposited lipid mixture: (□) PC:SM; (○) PC:Cho; and (Δ) SM-Cho

where A_{max} is the maximal absorbance at 492 nm and P_{50} is the concentration of toxin required to bind an amount equal to half the saturation value.

These data show a negligible binding to Cho. On the other hand, significant quantities of protein were bound to plates covered with PC or SM. In both cases, saturation is achieved when the concentration of the toxin is between 4 and 5 nM. The maximum amount of St II associated to SM covered plates is approximately 1.7 times that observed when PC is employed (Table 1). However, the P_{50} value is similar in both SM (ca. 0.58 nM) and PC (0.52 nM)

Table 1
Binding of St II of pure lipids and equimolar mixtures measured by ELISA and surface pressure experiments

Lipid composition	A^{I}_{max}	π_c (mN m^{-1})^{II}
SM	0.79±0.02^{c}	37.8±1.3
PC	0.46±0.04^{d}	29.7±1.4
Cho	0.05±0.01^{e}	32.6±1.6
PC–SM (50:50)	1.1±0.02^{a}	43.0±1.4
PC–Cho (50:50)	0.39±0.04^{d}	35.8±0.7
SM–Cho (50:50)	0.93±0.01^{b}	53.4±1.8

[I]Maximal absorbance at 492 nm, a measure of the amount of bound toxin in ELISA. Data show the average value ($n = 3$) and the SD. Different letters indicate differences among treatments ($p < 0.05$), according to Duncan's test for the means.
[II]Critical pressures determined by extrapolating regression lines from $\Delta\pi$ vs. π_0 plots ($r^2 > 0.94$, $n \geq 5$).

covered plates. The result of the total amount of St II bound at saturation being significantly larger for SM than for PC is compatible with the suggested preferential interaction between actinoporins and SM. In particular, it has been reported for sticholysins that exposure to SM reduces their HA (Alvarez-Valcárcel et al., 2001; Linder and Bernheimer, 1978) and that binding to PC liposomes is strongly promoted by SM addition (Tejuca et al., 1996). This result has been related to the possibility of specific binding between actinoporins and SM, both at the polar head and ceramide residue levels (Zecchini, 1994; Meinardi et al., 1995). On the other hand, the very low amount of St II bound to Cho-coated plates indicates that this lipid is unable to irreversibly bind the toxin. These results are compatible with a predominant role of phosphocholine binding sites in the irreversible association of the toxin to membranes (Mancheño et al., 2003).

Since it has been observed that St II binds more efficiently to vesicles comprising equimolar binary PC–SM mixtures than to the single components (Tejuca et al., 1996; Alvarez-Valcárcel et al., 2001), binding assays were performed with binary equimolar PC–SM, PC–Cho and SM–Cho mixtures. The results are shown in Fig. 1(B). These data indicate that SM containing mixtures show a considerably larger binding capacity than those comprising PC–Cho (significantly at the $p < 0.001$ level).

3.2. Incorporation to lipid monolayers

The increase in surface pressure elicited by the association of the toxin to previously formed lipid monolayers can be employed to characterize the ability of the toxin to interact with organized lipids. Control experiments showed that, at the employed concentration (0.93 μM), the toxin has a negligible effect on the surface tension of the air–water interface. Higher toxin concentrations are needed to detect its surface activity in the absence of lipids (Doyle et al., 1989).

The increase in surface pressure associated to the presence of the toxin was evaluated at several initial pressures of the lipid monolayer. These experiments were performed keeping the monolayer area constant. The increase in surface pressure at equilibrium as a function of the initial pressure in a SM monolayer, is shown in Fig. 2. Similar plots were obtained for PC, Cho and their mixtures. A suitable parameter for the characterization of the interaction is the critical pressure (π_c), obtained by extrapolating to zero the increase in pressure ($\Delta\pi$) as a function of the initial pressure (π_0). This parameter corresponds to the pressure that must be applied to avoid incorporation of the toxin to the monolayer and is directly correlated with the affinity of the toxin for the lipids in the monolayer (Brockman, 1999). The values obtained in the present work are shown in Table 1.

Regarding the pure lipids, the data in Table 1 show that the most favorable interaction (the highest π_c value) corresponds to SM containing

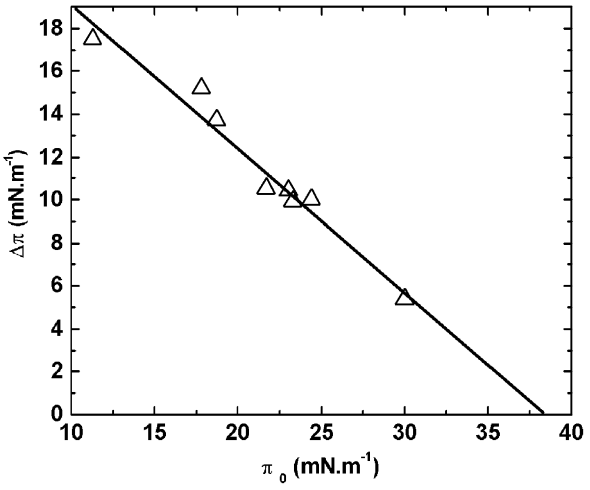

Fig. 2. Increase in surface pressure of a SM monolayer due to St II addition. $\Delta\pi$ values are plotted as a function of the initial monolayer pressure (π_0). Data obtained at 25 °C, pH = 7.5. St II concentration in the subphase: 930 nM. Reported values are those obtained after equilibration under gentle stirring. The line represents the best linear fit of the data ($r^2 = 0.96$).

systems with π_c values larger than 35 mN m^{-1}. This value corresponds to the lateral pressure of a typical biological membrane (Brockman, 1999). It has been proposed that, when π_c is higher than this critical limit, the protein not only associates to the monolayer, but penetrates it (Caaveiro et al., 2001). If π_c is lower than this value (PC, Cho) the association takes place without significant penetration of the toxin into the monolayer (Gutierrez-Aguirre et al., 2004).

Regarding the mixtures, the data in Table 1 show that both SM containing mixtures (PC–SM; SM–Cho) present π_c values considerably higher than 35 mN m^{-1}, and even higher than that of the SM monolayer, indicating a more favorable incorporation of St II to these mixed monolayers. The behavior of the SM–Cho mixture is particularly interesting since it presents a very high π_c, and the kinetics of the protein incorporation to this monolayer is considerably faster than those obtained in other systems (Fig. 3 and Table 2). These differences can be associated to preferential incorporation of the toxin to the interface of the condensed complexes present in SM–Cho containing monolayers (Barlic et al., 2004). Furthermore, the value of π_c in the PC–Cho mixture is near the 35 mN m^{-1} limit, being also higher than those of the pure components.

In order to further understand the behavior of the equimolar Cho containing mixtures, binary and ternary PC–SM–Cho monolayers of others compositions were studied. Typical data are given

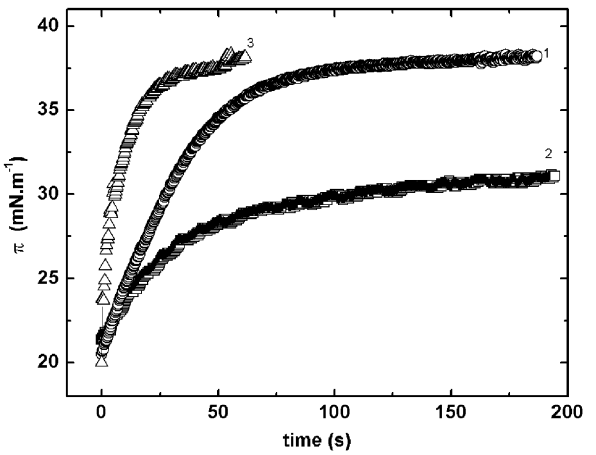

Fig. 3. Time profile of the increase in surface pressure following St II addition. Measurements were started immediately after St II (930 nM) injection to the subphase. Initial surface pressure: 20 mN m^{-1}. Lipid monolayer: (1) PC:SM (50:50); (2) PC:Cho (70:30); and (3) SM:Cho (60:40).

Table 2
Interaction of St II with binary and ternary lipid monolayers

Composition	v_{max} (s)^{I}	π_c (mN m^{-1})^{II}	m^{III}
PC:SM (50:50)	0.26±0.03^{c}	43.0±1.4	−0.73±0.04
PC:Cho (70:30)	0.22±0.07^{c}	32.2±0.8	−0.81±0.05
SM:Cho (60:40)	1.01±0.09^{a}	47.9±2.1	−0.56±0.04
SM:PC:Cho (50:35:15)	0.32±0.01^{c}	44.5±0.8	−0.71±0.03
SM:PC:Cho (50:15:35)	0.51±0.05^{b}	51.7±0.2	−0.61±0.01

^{I}Initial maximal rate of the surface pressure increase at an initial pressure of 20 mN m^{-1}. The values are the means of at least three measurements. Bold letters indicate different groups of values according to Duncan's test with $p<0.05$.
^{II}Critical pressure determined from $\Delta\pi$ vs. π_0 plots, like that shown in Fig. 2.
^{III}Slope of regression lines of the $\Delta\pi$ vs. π_0 plots ($r^2>0.96$; $n\geqslant 5$).

in Table 2. In this table, V_{max} corresponds to the initial (maximal) rate of surface pressure change, measured at an initial surface pressure of 20 mN m^{-1}, and derived from plots like those shown in Fig. 3. This pressure corresponds to an intermediate lipid packing, since the maximum pressure attainable in monolayers is nearly 48 mN m^{-1}, irrespective of their composition (data not shown). The values of m included in Table 2 correspond to the slope of the regression lines of $\Delta\pi$ vs. π_0 plots, such as that shown in Fig. 2.

The data in Table 2 show large differences in the values of the selected parameters among the different tested mixtures, and a fair degree of correlation between the measured parameters. In particular, high insertion rates are associated to high critical pressures and low absolute values of m. These trends are independent of the initial pressure of the monolayer. If it is accepted that high critical pressure values correspond to strong monolayer/toxin interactions (Caaveiro et al., 2001), the observed correlations would indicate that favorable interactions also increase the rate of the process. Representative examples of systems presenting high adsorption rates, high critical pressures and low absolute values of m are the SM:Cho (60:40) mixture and the ternary mixture rich in Cho (35%). On the other hand, the opposite situation is observed in the binary PC:Cho (70:30) mixture. The other mixtures show intermediate behaviors.

The analysis of the critical pressure values collected in Tables 1 and 2 allows, then to conclude that:

(i) All monolayers that do not contain SM have critical pressures equal or below 35 mN m^{-1};

(ii) Monolayers containing SM without or with low percentages of Cho (<35%) present intermediate values of the critical pressure; and
(iii) Monolayers containing SM and percentages of Cho equal to or larger than 35% present critical pressure values above 48 mN m^{-1}.

These results allow concluding that the interaction with the monolayers is particularly favorable when they contain SM and a large proportion of Cho. These results are qualitatively similar to those reported for the closely related actinoporin Eqt II by Barlic et al. (2004). These authors demonstrated that at low pressures the SM:PC:Cho (50:15:35) mixture forms two coexisting liquid phases in monolayers, with typically micrometer size domains that were readily observed using monolayer epifluorescence microscopy. Cho–SM interactions can be stabilized by hydrogen bonds between the 3β-OH group of Cho and the amide-linkage in SM (Slotte, 1999) favor a more ordered liquid phase. The presence of lipid microdomains seems to provide a particularly favorable arrangement of lipids for the association and function of the toxin.

3.3. Interaction of St II with liposomes

Lipid vesicles can be considered as the best model to mimic the behavior of natural membranes. These aggregates allow evaluating the toxin/protein association and the protein function by measuring the release of entrapped solutes.

A relevant property of vesicles is their fluidity, which is closely related to the bilayer phase state. These properties were estimated from Laurdan GP values and IR spectroscopy measurements. In Table 3, GP values and wavenumbers of CH_2-groups vibrations are shown. The high GP values obtained in Cho-rich mixtures can be ascribed to the presence of liquid ordered phases, predominant in bilayers containing more than 30% Cho, as suggested in closely related systems (Parassasi and Gratton, 1995; Patra et al., 1999; Veiga et al., 2001). Similar conclusions can be obtained from IR measurements, where the lowest wavenumber values correspond to SM containing vesicles with high Cho content.

Table 3
Generalized polarization of Laurdan (GP) and wavenumber of CH_2 groups in FTIR spectra (wn) measured in SUVs at 25 °C

Lipid composition	GP[a]	wn[b]
PC–SM (50:50)	0.13	2852.5
PC–Cho (70:30)	0.27	2853.1
SM–Cho (60:40)	0.6	2850.7
SM:PC:Cho (50:35:15)	0.4	2852.0
SM:PC:Cho (50:15:35)	0.57	2851.3

[a]GP measured in SUVs, according to Parasassi et al. (1990). Excitation was carried out at 340 nm, and the emission wavelengths were selected at 440 and 490 nm, respectively.
[b]Wavenumber at the maximum absorption of the band corresponding to the vibration of CH_2 groups of the lipid acyl chains.

The amount of unbound toxin in presence of liposomes was evaluated in ultrafiltration experiments carried out at a lipid/toxin ratio equal to 100 (St II 0.25 μM). Adsorption of the toxin to all SM containing vesicles was almost quantitative (>95%). Furthermore, this association was irreversible, as last as evidenced from HA determinations in the presence of vesicles (Bakás et al., 1996). Different results were obtained employing PC–Cho vesicles. In this system nearly 30% of activity was found in the ultrafiltrate. Furthermore, the association to these vesicles was reversible since no significant loss of activity was observed employing toxin pre-incubated with PC–Cho SUVs in HA determinations.

Association of the protein to SUVs was also assessed from changes in the intensity of the intrinsic protein fluorescence elicited by liposomes addition. After selective excitation of the Trp residues at 295 nm, the intensity of the emission is mainly conditioned by the exposition of these moieties to the external solvent. Hence, an increase in fluorescence is observed when the protein binds to the lipid bilayer. Typical data are shown in Fig. 4. The magnitude of the change, extrapolated to high lipid concentrations, measured by the parameter F_L/F_0, is related to the change of environment associated to the binding. It has been recently demonstrated by Mancheño et al. (2003), the aromatic patch exposed in the surface of the Eqt II molecule, together with electrostatic interactions, allow the initial anchorage of the protein to the membrane. Particularly, a critical role has been described for tryptophenyl residues 112 and 116 for EqT II, corresponding to Trp 110 and 114 in St II (Huerta et al., 2001). This could explain the significant changes observed in the microenvironment of these residues when the toxin associates to SM-containing vesicles (Table 4).

The lipid concentration over which the change is observed is related to the efficiency of the protein/

bilayer association. This was characterized by the Lip_{50} value, defined as the lipid concentration necessary to bind 50% of the protein.

Values of F_L/F_0 and Lip_{50} are collected in Table 4. In this table, K_{sv} values obtained employing acrylamide as fluorescence quencher are also included. These values were derived from the slopes of Stern–Volmer type plots, shown in Fig. 5.

The values collected in Table 4 show that PC:Cho vesicles behave differently than the other vesicles, regarding both the increase in fluorescence and K_{sv} values measured in the presence of the liposomes. Both results would indicate a low level of incorporation to those vesicles. In particular, the data indicate that St II binds very inefficiently to PC:Cho vesicles (large Lip_{50} value) and that the environment of the Trp groups is very little modified by this process (low F_L/F_0 value). These conclusions agree with the data obtained in the ultrafiltration and HA determinations in the presence of PC–Cho vesicles. A low degree of incorporation to PC–Cho layers is also stressed by the low critical pressure ($32.2\,mN\,m^{-1}$) measured for this mixture in the monolayer experiments (Table 2). In fact, there is a very good correlation ($r = 0.91$) between the values of F_L/F_0 and the critical pressure in the monolayers, suggesting that a common factor, the degree of interaction of the toxin with the bilayer, determines both processes.

The presence of Cho in SM containing liposomes favors the interaction process, particularly when it is

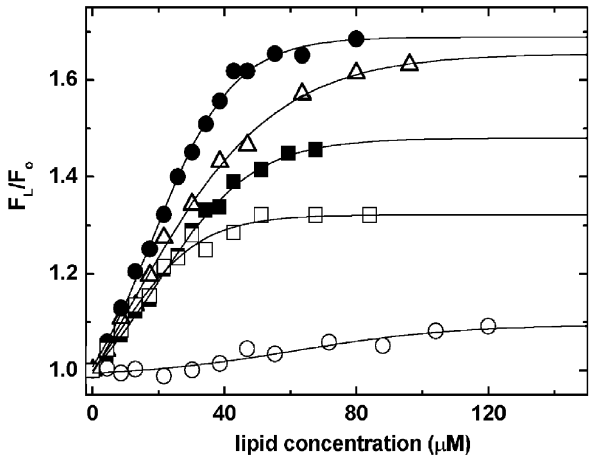

Fig. 4. Changes in the intrinsic protein fluorescence intensity as a function of the added lipid concentration. Data obtained with 0.7 μM toxin; excitation: 295 nm; emission: 335 nm. F_L represents the fluorescence at the given lipid concentration, and F_0 is the initial fluorescence intensity measured in the absence of vesicles: (□) PC:SM (50:50); (○) PC:Cho (70:30); (Δ) SM:Cho (60:40); (■) SM:PC:Cho (50:35:15); and (●) SM:PC:Cho (50:15:35).

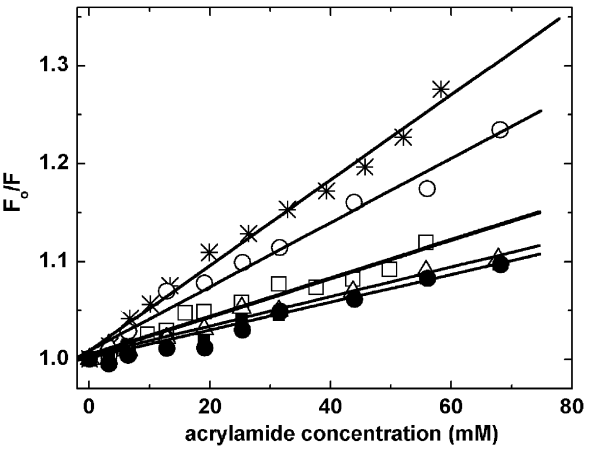

Fig. 5. Acrylamide quenching of the intrinsic St II fluorescence. Fluorescence intensities, measured in absence and in the presence of different vesicles (120 μM in lipids) are plotted according to the Stern–Volmer equation: (∗) buffer; (□) PC:SM (50:50); (○) PC:Cho (70:30); (Δ) SM:Cho (60:40); (■) SM:PC:Cho (50:35:15); and (●) SM:PC:Cho (50:15:35)

Table 4
Association of St II to small unilamellar vesicles (SUV)

Vesicle composition	F_L/F_0^{I}	Lip_{50} (μM)^{II}	n^{III}	10^2K_{sv} (M^{-1})^{IV}
Buffer	—	—	—	4.3
PC:SM (50:50)	1.34 ± 0.07^{b}	16.5	47	2.0
PC:Cho (70:30)	1.07 ± 0.01^{c}	70	200	3.3
SM:Cho (60:40)	1.60 ± 0.06^{a}	28	80	1.4
SM:PC:Cho (50:35:15)	1.4 ± 0.07^{b}	25	71	1.5
SM:PC:Cho (50:15:35)	1.57 ± 0.09^{a}	22	63	1.6

[I]Ratio between the fluorescence intensities from the bound and free protein. The data in Fig. 4 were fit to the best Boltzman function. ($\chi^2 < 1.72\times10^{-4}$). Bold letters indicate different groups of values according to Duncan's test with $p<0.05$.
[II]Amount of lipid necessary to bind half of the protein (0.7 μM total toxin concentration).
[III]Average number of lipid molecules per binding site estimated dividing Lip_{50} by half of the protein concentration in the assay.
[IV]Stern–Volmer constant obtained by regression analysis of data represented in Fig. 5 ($r^2 \geqslant 0.76$).

incorporated in high proportions. This is evidenced by the data obtained in SM:Cho (60:40) and SM:PC:Cho (50:15:35) liposomes. In these systems, the highest F_L/F_0 and lowest K_{sv} values are observed (Table 4), as well as the highest insertion rates and critical pressures in monolayers (Table 2). The kinetics of the association to the liposomes was not evaluated due to the fact that the process is almost complete in less than ca. 10 s.

The binding affinity and/or the number of binding sites at the liposome surface determine the values of Lip_{50}. The relevance of both factors depends on the interface degree of saturation and can be assessed by measuring the effect of the toxin concentration upon the Lip_{50} values. In the SM containing vesicles it was found that these values are nearly proportional to the toxin concentration (data not shown), suggesting that the process is limited by saturation of the vesicles. Therefore, the values of Lip_{50} can provide an estimation of the number of lipid molecules needed to generate a binding site (n), if we consider that the half of the toxin concentration is 0.35 μM.

The data in Table 4 show that the largest number of lipids required to generate a binding site (n) corresponds to PC–Cho (70:30) vesicles. On the other end, the smallest value of n corresponds to PC–SM (50:50) vesicles. This can be related with two different binding forms of the toxin to membrane: In the first case, the toxin interacts with a large number of lipids with low affinity, and even the interaction can be reversible. On the other hand, when the toxin is inserted into membrane, it interacts with a relatively smaller number of lipids, but with high affinity, making this binding irreversible.

The special role of SM can be related to the presence in this molecule of some groups with capacity to bind the toxin. Actinoporins interact with SM molecules both through the choline polar head (Meinardi et al., 1995; Mancheño et al., 2003) and the ceramide moiety (Zecchini, 1994). However, other factors, such as the accessibility to the toxin to the binding sites in SM and the presence of microdomains, may contribute to the number and strength of the binding sites. This statement is based on the observation that mixtures constitute better interfaces than those formed by pure compounds. In liposomes, this characteristic of mixtures has already been reported (Tejuca et al., 1996; Alvarez-Valcárcel et al., 2001; De los Ríos et al., 1998).

3.4. Permeabilization of vesicles

The time associated to the organization of the toxin in the bilayers, as well as the efficiency of the process, can be evaluated in dye releasing experiments. In the present work, this approach was applied using the ANTS–DPX system to monitor the rate and extent of the leakage process. At the employed lipid concentration (100 μM) and the lipid/toxin ratios ($\geqslant$100) one can consider that the toxin is almost quantitatively bound to the liposomes (Table 4). The only exception are PC:Cho vesicles, where fluorescence and ultrafiltration measurements show only a partial association to the vesicles.

The time course of the fluorescence intensity change following the addition of St II to a vesicle ensemble containing ANTS–DPX is shown in Fig. 6. If a single pore in a vesicle is enough to (instantaneously) lead to the total leakage of the entrapped fluorophore (Tejuca et al, 1996; De los Ríos et al., 1998), the final extent of the fluorescence increase elicited by the toxin addition is readily related to the fraction of vesicles in which at least one pore has been formed (f):

$$f = (F - F_0)/(F_{max} - F_0), \quad (3)$$

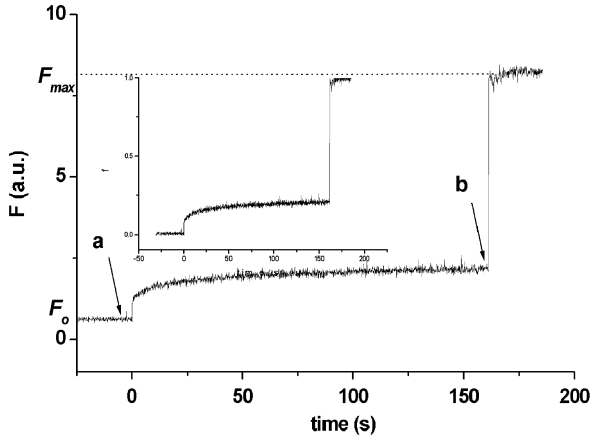

Fig. 6. Permeabilization of PC:SM vesicles elicited by St II addition followed by ANTS fluorescence increase. St II (23 nM) was added to 100 mM PC:SM LUVs and the increase in fluorescence (excitation 355 nm, emission 530 nm) and the fluorescence intensity measured thereafter at 25 °C under continuous stirring. Buffer: 10 mM Hepes, 200 mM NaCl, pH 7.5. Arrow (a) indicates the time of St II addition. Arrow (b) indicates the time of addition of a large excess of toxin. Inset: fraction of disrupted vesicles as a function of time. f values are calculated according to Eq. (3).

where F is the fluorescence at time t, F_0 the fluorescence prior to the toxin addition, and F_{max} the fluorescence intensity attained after addition of a large excess of protein.

Eq. (3) allows an estimation of the time course of pore formation in the vesicle ensemble (inset Fig. 6). If f_∞ is the fraction of permeabilized vesicles when the elapsed time is sufficiently long to disrupt all the pore bearing vesicles at a given protein concentration, $(1–f_\infty)$ measures the fraction of vesicles devoid of pores, at least during the time of the experiment. Values of f_∞ as a function of the toxin concentration are shown in Fig. 7. The value of f_∞ increases with protein concentration, and for a given lipid and toxin concentration, depends on the lipid composition. A remarkable feature of these data is that St II is able to generate pores in all the vesicles considered, even in the absence of SM (PC:Cho vesicles). This can be related to the promoting effect of Cho, since in pure PC vesicles, or in PC vesicles containing 30% phosphatidic acid or phosphatidylethanolamine, no significant permeabilization has been observed (Alvarez-Valcárcel et al., 2001).

In order to evaluate the number of pores formed, one can assume that the pores are randomly distributed in the vesicle population. In this case, Poisson distribution may be applied:

$$(1 - f_\infty) = \exp(-N), \tag{4}$$

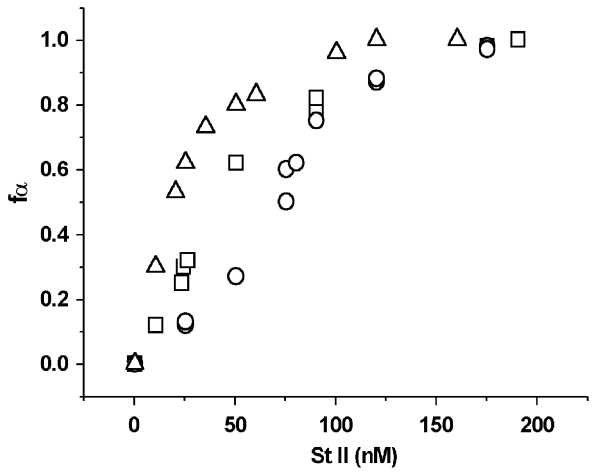

Fig. 7. Fraction of vesicles in which it has been formed at least one pore as a function of the initial toxin concentration. Lipid concentration: 0.1 mM. Values of f_∞ were calculated with Eq. (3) at long times (more than 10 min) after St II addition. Experiments were carried out as in Fig. 6: (□) PC:SM (50:50); (○) PC:Cho (70:30); and (Δ) SM:Cho (60:40).

where N is the average number of pores in the vesicle ensemble. Eq. (4) shows that N values can be derived from f_∞.

Assumption of a limited number of pores and a Poisson distribution requires a total, nearly irreversible association of the toxin to the liposomes. This condition applies to all tested systems but PC:Cho vesicles, as evidenced from binding experiments (ultrafiltration experiments and fluorescence in presence of liposomes, Fig. 4) and the HA inhibition experiments. Furthermore, the irreversibility of the process employing SM containing vesicles is also in agreement with the plateau observed in vesicle permeabilization experiments, as shown in Fig. 6 for PC:SM (see following discussion). Similar data were obtained employing other SM containing liposomes. On the other hand, all the data obtained employing PC:Cho vesicles indicate a partial and reversible association.

In order to compare the data obtained in different vesicles, the total number of formed channels in the different systems must be considered. This number can be obtained from the average number of channels per vesicle (N) if the total number of vesicles is known. This number can be estimated from the vesicle diameter (PC:SM (50:50), 108 nm; SM:Cho (60:40), 132 nm; SM:PC:Cho (50:35:15), 96 nm; SM:PC:Cho (50:15:35), 158 nm), the average surface covered by each lipid molecule, and the lipid concentration. Assuming that the bilayer width is 0.5 nm, and that the surfaces occupied by the lipids are 0.7 and 0.19 nm^2 for the phospholipids and Cho, respectively (Schechter, 1990), the average number of lipid molecules per vesicle (N_L) can be estimated. From this and the lipid concentration, the number of vesicles (N_{ves}) in each of the samples employed can be derived:

$$N_{ves} = N_{Av}[\text{Lipids}]/N_L. \tag{5}$$

The total number of pores (N_{pores}) is

$$N_{pores} = NN_{ves} \tag{6}$$

and the average number of St II molecules bound to the vesicle per generated pore (N_{StII}) is

$$N_{StII} = [\text{StII}]/N_{pores} \tag{7}$$

and hence

$$N_{pores} = (1/N_{StII})[\text{StII}]. \tag{8}$$

A plot of N_{pores}, calculated with Eq. (6), plotted against the total number of St II molecules should be linear and with a slope equal to the inverse of N_{StII}.

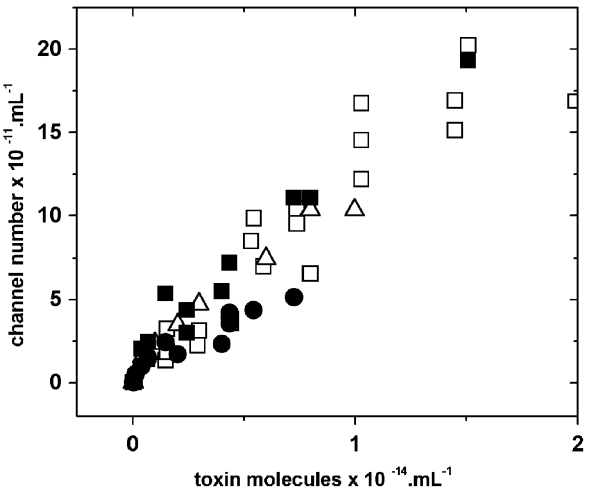

Fig. 8. Total number of formed channels as a function of the number of bound toxin molecules. The total number of channels was estimated from Eq. (6). (□)PC:SM (50:50); (Δ) SM:Cho (60:40); (■) SM:PC:Cho (50:35:15); and (●) SM:PC:Cho (50:15:35).

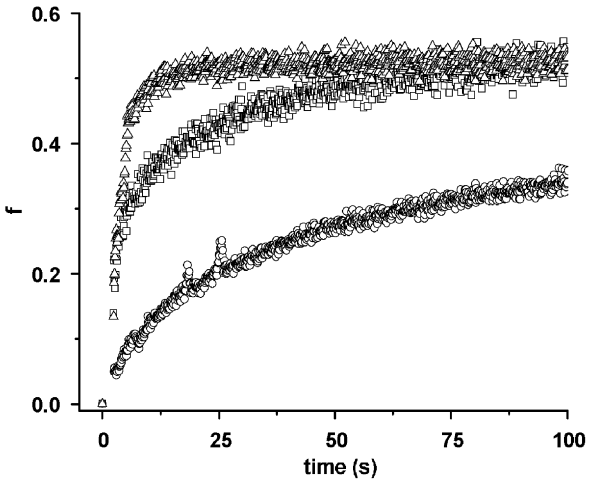

Fig. 9. Time profiles of vesicle permeabilization following St II addition. Protein concentrations were adjusted to obtain ca. 50% permeabilization at long times (5 min): (□) PC:SM (50:50) vesicles, St II = 48 nM; (○) PC:Cho (70:30) vesicles, St II = 82 nM; and (Δ) SM:Cho (60:40) vesicles, St II = 25 nM.

This type of plot is shown in Fig. 8. From this plot one can conclude that the efficiency of pore formation, defined as the number of toxins required to produce a pore (N_{StII}) is rather similar in all the vesicles, with nearly 80 toxins incorporated to the bilayer per pore produced in SM containing vesicles. This number is close to that previously reported for St I by Tejuca et al. (1996) in PC:SM 50:50 vesicles. If it is considered that only ca. four toxin molecules are involved in each pore (Tejuca et al., 1996), it implies that only a small fraction of the toxins associated to the membrane participates in pore formation (De los Ríos et al., 1998).

In all the systems including SM, there is, at low toxin concentrations, a fraction of undisrupted vesicles that remains almost constant for long periods of time (Fig. 9). This plateau is reached in spite of a large average number of toxins in each undisrupted vesicle. This population of remaining undisrupted vesicles could be explained in terms of the irreversibility of the vesicle–protein association in SM containing vesicles. On the other hand, in the PC–Cho (70:30) vesicles, there is a small residual permeabilization at longer times, compatible with an incomplete toxin association and reversibility of the association process, as previously discussed.

In order to have some insight regarding the relative rates of the pore formation process in the different vesicles, kinetics obtained under conditions leading to the same final fraction of permeabilized vesicles were compared. Typical results, obtained when the final fraction of permeabilized vesicles is 0.5, are shown in Fig. 9 and Table 5. In this table the time required to permeabilize 40% of the initial liposome ensemble ($t_{0.4}$) are shown. Similar results were obtained at a lower (0.2) fraction of permeabilized vesicles. Kinetic data could not be obtained at higher protein concentrations due to the extremely high rate of the process (data not shown).

Table 5
Amount of toxin needed to permeabilize 50% of the liposomes (100 μM in lipids) (C_{50}), and time required ($t_{0.4}$) to permeabilize 40% of the initial liposome ensemble

Composition	C_{50} (nM)[a]	$t_{0.4}$ (s)
PC:SM (50:50)	50	24
PC:Cho (70:30)	80	196
SM:Cho(60:40)	25	6.0
SM:PC:Cho (50:35:15)	90	11
SM:PC:Cho (50:15:35)	35	4.1

[a]Values obtained by curve fitting to data likethat shown in Fig. 7.

The results obtained regarding the kinetics of the process allow some generalizations. Under all the conditions, the kinetics of leakage from PC–Cho (70:30) vesicles is significantly slower and present a somehow different profile, a result explained in terms of a smaller degree of incorporation and the reversibility of the process. On the other end stand the SM–Cho vesicles that present the highest

permeabilization rates. It is interesting to note that the kinetic data in liposomes correlate with those regarding the rate of incorporation to monolayers. It can then be concluded that the factors favoring fast penetration to the monolayer also increase the rate of pore organization and/or penetration into the bilayer.

A good correlation exists between the rate of the pore forming process ($t_{0.4}$), and critical pressures ($r = -0.92$), F_L/F_0 ($r = -0.84$) and K_{sv} ($r = 0.98$) values. These correlations suggest that the rate of pore formation is determined by the same bilayer properties that allow deep penetration of St II and/or a strong interaction between the bilayer surface and the toxin. The rate of pore formation could be increased by microdomains present in Cho-rich SM-containing liposomes. The oligomerization process, in these conditions, would be kinetically favored and could constitute the main cause of the high rates of pore formation in Cho-rich liposomes.

A noticeable feature of the present data is that the characteristics of the membrane affect more the rate of channel formation (Fig. 9) than the total number of channels generated per toxin (Fig. 8). A plausible explanation could be that, in the toxin ensemble, only a small proportion of molecules can behave as "pore inductors" and/or be involved in pore formation (Gray et al., 1998). These competent conformations can be already present in the aqueous solution or be generated at the moment of (or after) the toxin-interface interaction. The presence of these molecules (or their aggregates) could explain both the lack of cooperativity in pore formation and the similarity of their efficiency in the different bilayers (Fig. 9).

4. Concluding remarks

The results of the present work are in agreement with previous results on liposomes (Alvarez-Valcárcel et al., 2001), SM presents the most favorable binding in ELISA and monolayer experiments. Regarding the role of Cho, the results allow concluding that the strength and rate of toxin–lipid interaction and the rate of functional organization of the toxin in bilayers are particularly favorable in lipid mixtures containing SM and high ($\geqslant 30\%$) Cho concentration. This conclusion is based on surface pressure (monolayers), fluorescence and permeabilization measurements. Data collected in Tables 1 and 2 show that, of all systems considered, only those with SM and large amounts of Cho present critical pressures higher than $48\,mN\,m^{-1}$. These mixtures present the fastest rates of surface pressure change after toxin addition (V_{max}), and the smallest absolute values of the slopes in surface pressure measurements (m), suggesting a particularly strong interaction between the toxin and the bilayers (Table 2). On the other extreme, SM lacking (PC:Cho) mixture presents the smallest rate of surface pressure change, the smallest critical pressure and the highest (negative) slope in the surface pressure experiments. These data are fully compatible with fluorescence measurements in liposomes, showing that the highest values of F_L/F_0, as well as the smallest K_{sv} correspond to liposomes containing SM and Cho (Table 4). In fact, there is a good correlation between both sets of results (π_c vs. F_L/F_0, $r = 0.91$, π_c vs. K_{sv}, $r = 0.92$).

The role of the SM in the interaction of St II with membranes is related to its capacity to bind the toxin irreversibly and in a very large extent. Nevertheless, its presence in the bilayers is not essential for pore formation. The presence of Cho in membranes formed by PC (in absence of SM) leads to pore formation (De los Ríos et al., 1998), even under circumstances where little toxin is associated to the lipids (Figs. 4 and 5). In this case, the permeabilizing activity of the protein takes place at lower rates compared to the membranes that contain the sphingolipid (Fig. 9).

The phase state of the membrane seems not to be the determinant factor in the interaction of St II with the lipids (Tables 3 and 4). The presence in the bilayers of the so called ordered-liquid phase characteristic of Cho-rich mixtures appears to favor both the interaction and function of the toxin.

Particularly, it was demonstrated that there are two different bound states depending on membrane lipid composition; the first of them occurs in membranes containing SM and is characterized by a large population of toxin irreversibly bound to the membrane with high affinity. The second one appears in membranes lacking SM where toxin binding is relatively low and reversible. Finally, permeabilization rate is mostly dependent on the population of bound toxin where only a small fraction of the bound toxin molecules are involved in pore formation.

Acknowledgements

This work was supported by a MUTIS fellowship (Asociación Española de Cooperación Internacional),

a CITMA (Cuba)–CONYCIT (Chile) collaboration program and IFS Grant no. F/3773-1. We thank Dr. Anselmo Otero for his help in ELISA.

References

Alvarez-Valcárcel, C.A., DallaSerra, M., Potrich, C., Bernhart, I., Tejuca, M., Martinez, D., Pazos, F., Lanio, M.E., Menestrina, G., 2001. Effect of lipid composition on membrane permeabilization by Sticholysin I and II, two cytolysins of the sea anemone *Stichodactyla helianthus*. Biophys. J. 80, 2761–2774.

Anderluh, G., Maček, P., 2002. Cytolytic peptide and protein toxins from sea anemones. Toxicon 40, 111–124.

Bakás, L., Ostolaza, H., Vaz, W., Goñi, F., 1996. Reversible and non reversible binding of *E. coli* hemolysin to lipid bilayers. Biophys. J. 71, 1876–1896.

Barlic, A., Gutiérrez-Aguirre, I., Caaveiro, J.M., Cruz, A., Ruiz-Argüello, M.B., Pérez-Gil, J., González-Mañas, J.M., 2004. On the active role played by the membrane during the insertion of equinatoxin-II, a pore-forming toxin from *Actinia equina*. J. Biol. Chem. 279, 34209–34216.

Bartlett, G.R., 1959. Phosphorus assay in column chromatography. J. Biol. Chem. 234, 466–468.

Bernheimer, A.W., Avigad, L.S., 1976. Properties of a toxin from the sea anemone *Stoichacis helianthus*, including specific binding to sphingomyelin. Proc. Natl. Acad. Sci. USA 73, 467.

Blumental, K.M., Kem, W.R., 1983. Primary structure of *Stoichactis helianthus* cytolysin III. J. Biol. Chem. 258, 5574.

Brockman, H., 1999. Lipid monolayers: why use half a membrane to characterize protein- membrane interactions? Curr. Opin. Struct. Biol 9, 438–443.

Caaveiro, J.M., Echabe, I., Gutierrez-Aguirre, I., Nieva, J.L., Arrondo, J.L.R., Gonzalez-Mañas, J.M., 2001. Differential interaction of equinotoxin II with model membranes in response to lipid composition. Biophys. J. 80, 1343–1353.

De los Ríos, V., Mancheño, J.M., Lanio, M.E., Oñaderra, M., Gavilanes, J.G., 1998. Mechanism of the leakage induced on lipid model membranes by the hemolytic protein Sticholysin II from the sea anemone *Stichodactyla helianthus*. Eur. J. Biochem. 252, 284–289.

Doyle, J.W., Kem, W.R., 1989. Binding of radiolabeled sea anemone cytolysin to erythrocyte membranes. Biochim. Biophys. Acta 987, 181–186.

Doyle, J.W., Kem, W.R., Vilallonga, F.A., 1989. Interfacial activity of an ion channel-generating protein cytolysin from the sea anemone *Stichodactyla helianthus*. Toxicon 27, 465–471.

Ellens, H., Bentz, J., Szoka, F.C., 1985. H^+ and Ca^{2+} induced fusion and destabilization of liposomes. Biochemistry 24, 3099–3106.

Gray, M., Szabo, G., Otero, A.S., Gray, L., Hewlett, E., 1998. Distinct mechanism for K efflux, intoxication and hemolysis by *Bordetella pertussis* AC toxin. J. Biol. Chem. 273, 18260–18267.

Gutierrez-Aguirre, I., Barlic, A., Podlesek, Z., Macek, P., Andelluh, G., Gonzalez-Mañas, J.M., 2004. Membrane insertion of the N-terminal α-helix of equinatoxin II, a sea anemone cytolytic toxin. Biochem. J. 384, 421–428.

Huerta, V., Morera, V., Guanche, Y., Chinea, G., Gonzalez, L.J., Betancourt, L., Martinez, D., Alvarez, C., Lanio, M.E., Besada, V., 2001. Primary structure of two cytolysin isoforms from Stichodactyla helianthus differing in their hemolytic activity. Toxicon 39, 1253–1256.

Kates, M., 1972. Techniques of Lipidilogy: Isolation, Analysis and Identification of Lipids. American Elsevier, Amsterdam, pp. 335–356.

Lakowicz, J.R., 1999. Principles of fluorescence spectroscopy. Kluwer Academic Plenum Publishers, New York, p. 698.

Lanio, M.E., Morera, V., Alvarez, C., Tejuca, M., Gomez, T., Pazos, F., Besada, V., Martinez, D., Huerta, V., Padron, G., Chavez, M.A., 2001. Purification and characterization of two hemolysins from *Stichodactyla helianthus*. Toxicon 39, 87–194.

Linder, R., Bernheimer, A.W., 1978. Effect of sphingomyelin-containing liposomes of phospholipase D from *Corinebacterium ovis* and the cytolysin from *Stoichactis helianthus*. Biochim. Biophys. Acta 530, 236–246.

Linder, R., Bernheimer, A.W., Kim, K.S., 1977. Interaction between sphingomyelin and a cytolysin from the sea anemone *Stoichactis helianthus*. Biochim. Biophys. Acta 467, 290.

Macek, P., Belmonte, G., Pederzolli, C., Menestrina, G., 1994. Mechanism of action of equinatoxin II, a cytolysin from the sea anemone *Actinia equina* L. belonging to the family of actinoporins. Toxicology 87, 205–227.

Mancheño, J.M., Martin-Benito, J., Martinez-Ripoll, M., Gavilanes, J.G., Hermoso, J.A., 2003. Crystal and electron microscopy structures of sticholysin II actinoporin reveal insights into the mechanism of membrane pore formation. Structure 11, 1319–1328.

Martínez, D., Campos, A.M., Pazos, F., Álvarez, C., Lanio, M.E., Casallanovo, F., Schreier, S., Salinas, R.K., Vergara, C., Lissi, E., 2001. Properties of St I and St II, two isotoxins isolated from *S. helianthus*: a comparison. Toxicon 39, 1547–1560.

Mayer, L.D., Hope, M.J., Cullis, P.R., 1986. Vesicles of variable size produced by a rapid extrusion procedure. Biochim. Biophys. Acta 858, 161–168.

Meinardi, E., Florin-Christensen, M., Paratcha, G., Azcurra, J.M., Florin-Christensen, J., 1995. The molecular basis of the self non self selectivity of a coelenterate toxin. Biochem. Biophys. Res. Commun. 216, 348–354.

Muga, A., Mantsch, H.H., Surewicz, W.T., 1991. Apocytochrome *c* interaction with phospholipids membranes studied by Fourier-transform infrared spectroscopy. Biochemistry 30, 2629–2635.

Parassasi, T., Gratton, E., 1995. Membrane lipid domains and dynamics as detected by Laurdan fluorescence. J. Fluoresc. 5, 59–69.

Parasassi, T., De Stasio, G., d'Ubaldo, A., Gratton, E., 1990. Phase fluctuation in phospholipid membranes revealed by Laurdan fluorescence. Biophys. J. 57, 1179–1186.

Patra, S.K., Alonso, A., Arrondo, J.L.R., Goñi, F., 1999. Liposomes containing sphingomyelin and cholesterol: detergent solubilization and infrared spectroscopic studies. J. Liposome Res. 9, 247–260.

Pico, M.C., Basulto, A., Del Monte, A., Hidalgo, A., Lanio, M.E., Alvarez, C., Felicó, E., Otero, A., 2004. Cross-reactivity and inhibition of haemolysis by polyclonal antibodies raised against St II, a cytolysin from the sea anemone *Stichodactyla helianthus*. Toxicon 43, 167–171.

Schechter, E., 1990. Biochimic et Biophysique des membranes. Aspects structuraux et fonctionnels, Paris, Masson, p. 414.

Shin, M.L., Michaels, D.W., Mayer, M.M., 1979. Membrane damage by a toxin from the sea anemone *Stoichactis helianthus*. II. Effect of membrane lipid composition in a liposome system. Biochim. Biophys. Acta 555, 79.

Slotte, J.P., 1999. Sphingomyelin–cholesterol interactions in biological and model membranes. Chem. Phys. Lipids 102, 13–27.

Stevens Jr., S.M., Kem, W.R., Prokai, L., 2002. Investigation of cytolysin variants by peptide mapping: enhanced protein characterization using complementary ionization and mass spectrometric techniques. Rapid Commun. Mass Spectrom. 16, 2094.

Tejuca, M., DallaSerra, M., Ferreras, M., Lanio, M.E., Menestrina, G., 1996. Mechanism of membrane permeabilization by Sticholysin I, a cytolysin isolated from the venom of the sea anemone *Stichodactyla helianthus*. Biochemistry 35, 14947–14957.

Tejuca, M., Anderluh, G., Macek, P., Marcet, R., Torres, D., Sarracent, J., Alvarez, C., Lanio, M.E., Dalla Serra, M., Menestrina, G., 1999. Antiparasite activity of sea-anemone cytolysins on *Giardia duodenalis* and specific targeting with anti-Giardia antibodies. Int. J. Parasitol. 29, 489–498.

Tejuca, M., Dalla Serra, M., Potrich, C., Alvarez, C., Menestrina, G., 2001. Sizing the radius of the pore formed in erythrocytes and lipid vesicles by the toxin sticholysin I from the sea anemone *Stichodactyla helianthus*. J. Membr. Biol. 183, 125–135.

Tejuca, M., Díaz, I., Figueredo, R., Roque, L., Pazos, F., Martínez, D., Iznaga-Escobar, N., Pérez, R., Alvarez, C., Lanio, M.E., 2004. Construction of an immunotoxin with the pore forming protein StI and ior C5, a monoclonal antibody against a colon cancer cell line. Int. Immunopharmacol. 4, 731–744.

Veiga, M.P., Arrondo, J.L., Goñi, F.M., Alonso, A., Marsh, D., 2001. Interaction of cholesterol with sphingomyelin in mixed membranes containing phosphatidylcholine, studied by spin-label ESR and IR spectroscopies. A possible stabilization of gel-phase sphingolipid domains by cholesterol. Biochemistry 40, 2614–2622.

Yamaji, A., Sekizawa, Y., Emoto, K., Sakuraba, H., Inoue, K., Kobayashi, H., Umeda, M., 1998. Lysenin, a novel shingomyelin-specific binding protein. J. Biol. Chem. 273, 5300–5306.

Zecchini, M., 1994. Struttura e funzione di una citolisina basica estratta dalle nematocisti dell' anemone di mare Actinia equina. Tesi di laurea in Scienze Biologiche Universitá degli studi di Padova, Italia.